Time-Dependent Elastic Properties and Lattice Temperature of the Photoexcited Iron Oxide Nanocrystals

Tai-Yen Chen, Chih-Hao Hsia, and Dong Hee Son*

Department of Chemistry, Texas A&M University, College Station, Texas 77842

Received: March 20, 2008; Revised Manuscript Received: April 17, 2008

Time-dependent elastic properties and lattice temperature of the photoexcited superparamagnetic iron oxide (Fe_3O_4) nanocrystals were investigated by pump/probe transient absorption measurements. Information on the elastic property and lattice temperature of the photoexcited nanocrystals was obtained from the period of coherent acoustic phonon. From the excitation fluence-dependent measurement of the coherent phonon period, initial temperature rise due to the photoexcitation was estimated. From the two-pump/probe transient absorption measurement, where the first pump heated the lattice and the time-delayed second pump generated coherent phonon, time dependence of the lattice temperature was also investigated. Implication of knowledge on the lattice heating and cooling on the study of the magnetization dynamics of the photoexcited magnetic nanocrystals was discussed.

1. Introduction

Nanoscale magnetic materials have been attracting much attention in recent years due to the wide range of technological applications ranging from biomedical imaging to magnetic data storage devices.[1–4] Chemically synthesized colloidal magnetic nanocrystals are serving as a particularly useful material platform in many studies for a variety of reasons. Easy control of the size, morphology and stoichiometry, and facile chemical functionalization enabled systematic studies of the magnetic properties in nanometer length scale in diverse chemical environments.[5–8] Recently, optically induced dynamic magnetization in magnetic nanocrystals has been gaining interest due to the potential applications in high-density and high-speed magnetic data storage devices.[9,10] Optical manipulation of magnetization by using femtosecond laser pulses on bulk surfaces has been extensively investigated in the past decade. Various mechanisms of thermal and nonthermal optical control of the magnetization were proposed from these earlier studies.[11–14] The coupled nature of the magnetization dynamics to the dynamics in electronic and lattice degrees of freedom has also been investigated in these studies. For instance, optically induced demagnetization in ferromagnetic metals has often been explained phenomenologically by using the three-temperature model.[15] This model described the time evolution of the magnetization in terms of the equilibration of the electronic, lattice, and spin temperatures. Modulation of the magnetization by coherent phonon on the subpicosecond time scale was also observed, which demonstrated the presence of the ultrafast coupling pathway between the spin and lattice degrees of freedom.[16]

The fundamental mechanisms of optical manipulation of the magnetization and the nature of the coupling among the electronic, lattice, and spin degrees of freedom should be the same regardless of the dimension of the magnetic materials. However, the dynamic magnetization in nanocrystals can exhibit a dependence on the size unlike that in the bulk phase. In principle, variation of the size of magnetic nanocrystals can influence the dynamics in spin degrees of freedom directly or indirectly through the coupling of the

spin to the electronic and lattice degrees of freedom. For instance, size dependent magnetization dynamics in iron oxide nanocrystals discussed in our earlier work proposed the size-dependent spin correlation as its origin.[17] On the other hand, size dependence of the lattice temperature due to different lattice cooling rates may also result in size-dependent magnetization, especially when the thermal excitation of spins becomes important. Therefore, it will be important to obtain an understanding of the energy dissipation in electronic and lattice degrees of freedom to obtain an accurate picture of the dynamic magnetization in photoexcited magnetic nanocrystals.

In this study, we investigated the elastic property and the lattice temperature of the photoexcited iron oxide (Fe_3O_4) nanocrystals as the prototypical magnetic ferrite nanocrystals. Information on the elastic properties and lattice temperature was obtained by measuring the period of coherent acoustic phonon as a function of excitation fluence and delay time after the excitation. The period of the radial breathing mode of the coherent acoustic phonon in spherical nanocrystals is determined by sound velocity and the radius of the nanocrystal according to a simple model based on Lamb's theory.[18] Therefore, information on the elastic property can be obtained from the measurement of the period of coherent acoustic phonon. A rough estimation of the lattice temperature after the excitation was made from the knowledge of temperature-dependent sound velocity in a closely related ferrite material. The time-dependent period of coherent acoustic phonon was also measured by employing the two-pump/probe measurement, where the first pump pulse acted as a heating pulse and the weaker second pump pulse created coherent phonon at various delay times. From this measurement, the time-dependent lattice temperature of the photoexcited Fe_3O_4 nanocrystals was estimated.

2. Experimental Section

Colloidal iron oxide nanocrystals (Fe_3O_4) were synthesized by following the published procedure.[5] Briefly, Fe_3O_4 nanocrystals were synthesized by reducing Fe(acetylacetonate)$_3$ with a mixture of oleic acid, oleylamine, and 1,2-dodecandiol
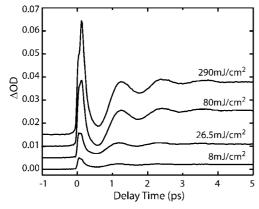

Figure 1. Pump/probe transient absorption data of colloidal Fe_3O_4 nanocrystals obtained with 780 nm pump and 550 nm probe at various excitation fluences.

at 290 °C in benzyl ether. Nanocrystals of different sizes were prepared by controlling the synthesis temperature and reaction time. The size and structure of the resulting sample were characterized by transmission electron microscopy (TEM) and powder X-ray diffraction (XRD). According to the analysis of vis−NIR absorption spectra of the sample, the final samples used in the experiment were more oxidized than the Fe_3O_4 nanocrystals initially synthesized. The nanocrystal samples used in all the measurements were dispersed in cyclohexane. The sample solutions were continuously circulated through a flat nozzle to create a 400 μm-thick jet of the sample solutions. The free streaming jet of samples with a linear flow speed of 2−3 m/s was used to prevent potential sample damage from repeated exposure of the sample on the same sample region. The concentrations of the nanocrystal samples were adjusted such that total Fe ion concentration was kept approximately at 1.8 mM. Inductively coupled plasma atomic emission spectroscopy was employed to measure the Fe ion concentration of the nanocrystal sample solutions.

Pump/probe transient absorption traces of the nanocrystal samples were recorded with an amplified Ti:Sapphire laser system, which produced pulses of 60 fs centered at 780 nm with a 3 kHz repetition rate. The laser beam was split to two beams for the usual pump/probe measurement, where one was used as the pump and the other was used to generate the white light continuum probe. For the two-pump/probe experiment, the intensity ratio of the two pump beams was set to 90:10 by using a beam splitter. The white light continuum used as the probe was generated by focusing $\sim$2 μJ of 780 nm pulses on a 2 mm-thick sapphire crystal. The probe beam passed through a prism dispersion compensator, which was also used to preselect the wavelength of the probe light before the sample. Typical pump/probe cross correlation and time step were 70 and 5 fs, respectively. Pump and probe beam diameters were 150 and 30 μm, respectively. For the excitation fluence-dependence experiment, the excitation fluence was varied up to 290 mJ/cm^2.

3. Results and Discussion

3.1. Excitation Fluence-Dependent Elastic Property and the Lattice Temperature. Figure 1 shows the pump/probe transient absorption (ΔOD) data of colloidal Fe_3O_4 nanocrystal samples (4.8 nm in diameter) at various pump fluences obtained with 780 nm pump and 550 nm probe light. With increasing excitation fluence, the amplitudes of both the oscillatory and

nonoscillatory components increased. The oscillatory component is due to coherent acoustic phonon, which has been observed in many nanocrystalline materials including semiconductor and metal nanocrystals.[19,20] In the case of Fe_3O_4 nanocrystals excited at 780 nm, coherent phonon is probably generated by the displacive mechanism from intervalence charge transfer transition between Fe^{2+} and Fe^{3+} ions.

Nanocrystal samples of two different sizes (4.8 and 8.4 nm in diameter) were used for the measurement of the excitation fluence-dependent period and amplitude of coherent acoustic phonon. For both samples, concentration of the total Fe ions in nanocrystal solution was maintained approximately the same. On the basis of the measurement of the pump beam absorption by the sample solution, the average excitation density per nanocrystal was also similar in both samples. To obtain the amplitude (a_o) and period (τ) of the oscillation due to coherent phonon, the transient absorption data (ΔOD) were fit to the sum of multiexponential functions and an exponentially decaying cosine function as shown in eq 1.

$$\Delta OD(t) = \sum a_i \exp(t/\tau_i) + a_o \cos(2\pi t/\tau + \varphi) \exp(-t/\tau_o)$$

(1)

The extracted period and amplitude of the oscillation as a function of the excitation fluence for two nanocrystal samples are shown in Figure 2a−c. The period (τ) is shorter for the smaller nanocrystal as predicted from a model based on Lamb's theory.[18] In spherical nanocrystals, the period of coherent acoustic phonon corresponding to the radial breathing mode is related to the radius (r) and sound velocity of the nanocrystal as shown in eq 2,

$$\tau = \frac{2\pi r}{\eta c_L}, \quad \eta \cot(\eta) = 1 - \left(\frac{\eta c_L}{2 c_T}\right)^2$$

(2)

where c_L and c_T are the longitudinal and transverse velocity of sound, respectively, which are related to Young's modulus (C_{11} and C_{44}) and density (ρ) through $c_L = (C_{11}/\rho)^{1/2}$ and $c_T = (C_{44}/\rho)^{1/2}$.

With the increasing excitation fluence, the period of coherent phonon increased as shown in Figure 2a,b. This is most likely due to the heating of the lattice by photoexcitation resulting in the softening of the lattice. A similar fluence dependence of the coherent phonon period was observed previously in metallic nanocrystals, where the increase of the coherent phonon period was attributed to the lattice heating.[21] Nonthermal softening of the lattice is not likely to play a significant role, since the effect of the excitation on the period of coherent acoustic phonon persists much longer ($>$100 ps) than would be expected from a purely electronic origin.[22] More detailed discussion on the time dependence of coherent phonon will be made in the following section. The amplitude of oscillation also increases with increasing excitation fluence as shown in Figure 2c. The amplitude of oscillation increases linearly to the excitation fluence up to 100 mJ/cm^2 and saturated at higher fluences. A similar increase of the amplitude with the excitation fluence was observed in semiconductor nanocrystals as well.[23] The increase of the oscillation amplitude with the excitation fluence can be interpreted as the increasing magnitude of lattice displacement, although there is not a simple and quantitative relationship between the oscillation amplitude of ΔOD and lattice displacement.

The fractional change of the period at fluence F with respect to the period extrapolated to zero fluence, $[\tau(F) - \tau(0)]/\tau(0)$, is

Photoexcited Iron Oxide Nanocrystals

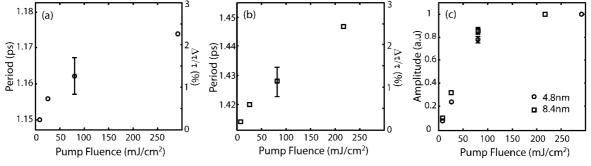*J. Phys. Chem. C, Vol. 112, No. 27, 2008* **10127**

Figure 2. Excitation fluence dependence of coherent phonon period for 4.8 (a) and 8.4 nm (b) nanocrystals. A typical error bar is shown on each panel. On the right *y*-axes of panels a and b, $\Delta\tau/\tau$ represents the fractional change of period $[\tau(F) - \tau(0)]/\tau(0)$ described in the text. (c) Excitation fluence dependence of the amplitude of oscillation in transient absorption data. The amplitudes are normalized to the maximum value for the nanocrystals of both sizes.
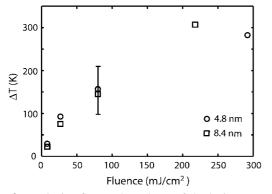

Figure 3. Excitation fluence dependence of the lattice temperature estimated from the period of coherent phonon. The error bar shown in the figure is a typical value.

indicated on the right *y*-axes of panels a and b of Figure 2. Both samples exhibit a very similar fluence dependence of the fractional change of period, indicating that the effect of excitation on the elastic constants is comparable in both samples. This may not be surprising since approximately the same excitation densities in both samples will result in the lattice heating to a comparable level if the cooling of the lattice at early delay time is ignored.

The excitation fluence-dependent period of coherent acoustic phonon is due to the temperature dependence of longitudinal and transverse sound velocities according to eq 2. For a majority of the materials, sound velocity can be approximated as a linearly decreasing function of temperature.[24] Therefore, the data shown in Figure 2 can be used to estimate the average lattice temperature if temperature-dependent sound velocity is known. Unfortunately, the data for temperature-dependent sound velocity are not available for Fe_3O_4 above 300 K, making the direct determination of the lattice temperature from the present experimental data difficult. Nevertheless, a rough estimate of the lattice temperature has been made by using the temperature-dependent sound velocity of $MgFe_2O_4$, which has the same cubic spinel structure as Fe_3O_4 with only 0.3% difference in the lattice parameter. The temperature dependence of the coherent phonon period calculated for $MgFe_2O_4$ was decreasing almost linearly to the temperature. From the comparison of the calculated fractional changes of the coherent phonon period at temperature *T*, $[\tau(T) - \tau(294K)]/\tau(294K)$, with $[\tau(F) - \tau(0)]/\tau(0)$ displayed in Figure 2, a rough estimate of the average lattice temperature was made. Figure 3 shows the excitation fluence dependence of the lattice temperature estimated as described above for both nanocrystal samples.

This analysis indicates that the temperature rise (ΔT) of the lattice can be 300 K after the excitation at the highest excitation fluence of this study. The theoretical maximum ΔT, if the energy of all the absorbed photons is released as heat, is calculated to be 800 K under the same excitation fluence.[25] Actual temperature rise will be less than 800 K due to the finite time scale of the electronic relaxation and heat dissipation from the lattice to the surroundings. Considering the uncertainty in the temperature-dependent sound velocity used, ΔT of 300 K seems a reasonable estimate for the temperature rise by the photoexcitation. Since the intervalence charge transfer transition centered at 1.5 μm was excited with a 780 nm pump pulse, such a temperature rise in the lattice may be possible from the rapid energy relaxation in the excited state.

3.2. Time-Dependent Elastic Property and Lattice Temperature. To obtain information on the time-dependent elastic property and the lattice temperature after the excitation, pump/probe transient absorption was measured employing two pump pulses. The first pump pulse with fluence of 265 mJ/cm^2 was used as the heating pulse. The second, weak pump pulse was used as the excitation pulse generating coherent phonon at various delay times with respect to the first pump pulse. The combined energy of both pump pulses was 290 $mJ/cm.^2$ The probe pulse with a variable time delay with respect to the second pump pulse recorded the transient absorption data. Typical two-pump/probe transient absorption data from 8.4 nm samples are shown in Figure 4a. The period of the oscillation following the second pump pulse was extracted from the fitting of the data as described in the previous section. Figure 4b shows the period of coherent acoustic phonon at various time delays between the two pump pulses. The increased coherent phonon period due to the heating pulse recovered continuously as the time delay between the two pump pulses increased.

The recovery of the coherent phonon period with time represents the cooling of the lattice via dissipation of the heat to the surrounding solvent medium. The time-dependent temperature of the lattice was estimated from the time-dependent period of coherent phonon as described in the previous section. The temperature scale is indicated on the right *y*-axis of Figure 4b. Although the number of data points is limited to reliably extract the time scale of lattice cooling, the lattice temperature recovered by about 40% after 100 ps. According to the earlier studies on the time-dependent lattice temperature of the photoexcited metal colloidal nanocrystals, the time scale of the temperature decay was relatively well described by a simple heat dissipation model: a sphere im-
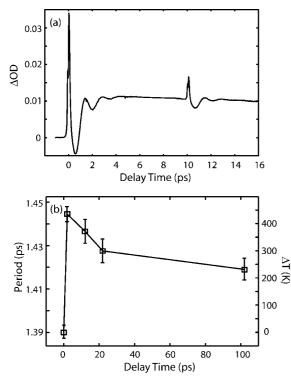
Figure 4. (a) Transient absorption data from the two-pump/probe measurement. (b) Time dependence of the coherent phonon period and the estimated lattice temperature obtained from the two-pump/probe measurement.

mersed in an infinite bath.[20,26] The following simple expression has been used to estimate the characteristic time scale for the heat dissipation (τ_d) in the limit of no interface effect on thermal conductance:[27]

$$\tau_d = \frac{r^2 C_p^2}{9 C_f \Lambda_f} \tag{3}$$

where r and C_p are the radius and heat capacity per unit volume of the particle, respectively. C_f and Λ_f are the heat capacity per unit volume and thermal conductivity of the fluid respectively. Although the temperature of the lattice in a real situation does not decay exponentially and τ_d sets only a lower limit to the time scale the temperature decay, eq 3 can still give useful insight into the rate of heat dissipation in the nanocrystals. By using the literature value of $C_p = 3.22$ J/(cm^3·K), $C_f = 1.44$ J/(cm^3·K), and $\Lambda_f = 0.123$ W/(m·K),[28,29] τ_d is calculated to be 110 ps for 8.4 nm Fe$_3$O$_4$ nanocrystals dispersed in cyclohexane. Considering the neglected effect of the finite interfacial heat conductance, the experimentally measured time scale of the lattice temperature decay is in reasonable agreement with the calculation, using a crude model.

The result from this study can be applied, for instance, to assist the interpretation of the data from our earlier studies on the size-dependent magnetization dynamics in optically excited Fe$_3$O$_4$ nanocrystals.[17] A strongly size-dependent amplitude of the optically induced demagnetization in Figure 5 of ref 17 was obtained at the excitation fluence of 50 mJ/cm^2. On the basis of the result from this study, the temperature rise (ΔT) in the nanocrystal at 100 ps is estimated to be about 50 K for 8.4 nm nanocrystals. Such a temperature rise in the lattice is too small to explain the observed size-dependent demagnetization amplitude on ~100 ps time scale in terms of thermal excitation of spins by the heated lattice with the size-dependent cooling rate.[30] Therefore, the pos-

sibility of the heated lattice with the size-dependent cooling rate being the origin of the size-dependent magnetization dynamics can be eliminated.

4. Conclusion

Excitation fluence and the time-dependent elastic property and lattice temperature of the photoexcited colloidal magnetic nanocrystals were investigated by employing transient absorption spectroscopy. The period of coherent acoustic phonon was extracted by fitting the oscillatory feature of the transient absorption data to an exponentially decaying cosine function. Since the period of the coherent acoustic phonon is determined by the elastic constants, the lattice temperature was estimated from the temperature dependence of the elastic constants. Time-dependent lattice temperature was also estimated by employing the two-pump/probe technique, where the first pump pulse acted as a heating pulse and the weaker second pump pulse created coherent phonon at various delay times. Information on the excitation fluence and time-dependent lattice temperature obtained in this study will be important in the investigation of optically induced dynamic magnetization and thermal transport in magnetic nanocrystals.

References and Notes

(1) Lee, J. H.; Huh, Y. M.; Jun, Y.; Seo, J.; Jang, J.; Song, H. T.; Kim, S.; Cho, E. J.; Yoon, H. G.; Suh, J. S.; Cheon, J. *Nat. Med.* **2007**, *13*, 95.
(2) Prinz, G. A. *Science* **1998**, *282*, 1660.
(3) Zhang, G. P.; Hübner, W. *Phys. Rev. Lett.* **2000**, *85*, 3025.
(4) Wolf, S. A.; Awschalom, D. D.; Buhrman, R. A.; Daughton, J. M.; von Molnar, S.; Roukes, M. L.; Chtchelkanova, A. Y.; Treger, D. M. *Science* **2001**, *294*, 1488.
(5) Sun, S.; Zeng, H. *J. Am. Chem. Soc.* **2002**, *124*, 8204.
(6) Park, J.; An, K. J.; Hwang, Y. S.; Park, J. G.; Noh, H. J.; Kim, J. Y.; Park, J. H.; Hwang, N. M.; Hyeon, T. *Nat. Mater.* **2004**, *3*, 891.
(7) Song, Q.; Zhang, Z. J. *J. Phys. Chem. B* **2006**, *110*, 11205.
(8) Redl, F. X.; Black, C. T.; Papaefthymiou, G. C.; Sandstrom, R. L.; Yin, M.; Zeng, H.; Murray, C. B.; O'Brien, S. P. *J. Am. Chem. Soc.* **2004**, *126*, 14583.
(9) Buchanan, K. S.; Zhu, X. B.; Meldrum, A.; Freeman, M. R. *Nano Lett.* **2005**, *5*, 383.
(10) Andrade, L. H. F.; Laraoui, A.; Vomir, M.; Muller, D.; Stoquert, J. P.; Estournes, C.; Beaurepaire, E.; Bigot, J. Y. *Phys. Rev. Lett.* **2006**, *97*, 127401.
(11) Ju, G. P.; Hohlfeld, J.; Bergman, B.; van de Veerdonk, R. J. M.; Mryasov, O. N.; Kim, J. Y.; Wu, X. W.; Weller, D.; Koopmans, B. *Phys. Rev. Lett.* **2004**, *93*, 197403.
(12) Rhie, H. S.; Durr, H. A.; Eberhardt, W. *Phys. Rev. Lett.* **2003**, *90*, 247201.
(13) Kimel, A. V.; Kirilyuk, A.; Usachev, P. A.; Pisarev, R. V.; Balbashov, A. M.; Rasing, T. *Nature* **2005**, *435*, 655.
(14) Stamm, C.; Kachel, T.; Pontius, N.; Mitzner, R.; Quast, T.; Holldack, K.; Khan, S.; Lupulescu, C.; Aziz, E. F.; Wietstruk, M.; Durr, H. A.; Eberhardt, W. *Nat. Mater.* **2007**, *6*, 740.
(15) Beaurepaire, E.; Merle, J. C.; Daunois, A.; Bigot, J. Y. *Phys. Rev. Lett.* **1996**, *76*, 4250.
(16) Melnikov, A.; Radu, I.; Bovensiepen, U.; Krupin, O.; Starke, K.; Matthias, E.; Wolf, M. *Phys. Rev. Lett.* **2003**, *91*, 227403.
(17) Hsia, C. H.; Chen, T. Y.; Son, D. H. *Nano Lett.* **2008**, *8*, 571.
(18) Lamb, H. *Proc. Math. Soc. London* **1882**, *13*, 187.
(19) Krauss, T. D.; Wise, F. W. *Phys. Rev. Lett.* **1997**, *79*, 5102.
(20) Hu, M.; Hartland, G. V. *J. Phys. Chem. B* **2002**, *106*, 7029.
(21) Hu, M.; Petrova, H.; Hartland, G. V. *Chem. Phys. Lett.* **2004**, *391*, 220.
(22) Hunsche, S.; Wienecke, K.; Dekorsy, T.; Kurz, H. *Phys. Rev. Lett.* **1995**, *75*, 1815.
(23) Son, D. H.; Wittenberg, J. S.; Banin, U.; Alivisatos, A. P. *J. Phys. Chem. B* **2006**, *110*, 19884.
(24) *Handbook of Elastic Properties of Solids, Liquids, and Gases, Volume 3: Elastic Properties of Solids: Biological and Organic Materials, Earth and Marine Sciences*, 2001.

Photoexcited Iron Oxide Nanocrystals

J. Phys. Chem. C, Vol. 112, No. 27, 2008 **10129**

(25) This value was obtained from the total number of nanocrystals (4.26 × 10⁹ particles) and the absorbed photon energy (4.39 × 10⁻⁷ J) within the probe beam volume (2.83 × 10⁻⁷ cm³) and bulk heat capacity of Fe_3O_4 (0.643 J/(mol·K)) by assuming fast heating and slow cooling of the lattice.

(26) Cooper, F. *Int. J. Heat Mass Transfer* **1977**, *20*, 991.

(27) Wilson, O. M.; Hu, X.; Cahill, D. G.; Braun, P. V. *Phys. Rev. B* **2002**, *66*, 224301.

(28) BialkowskiS. E. *Photothermal Spectroscopy Methods for Chemical Analysis*; John Wiley: New York, 1996; Vol. 134.

(29) Razzaq, M. Y.; Anhalt, M.; Frormann, L.; Weidenfeller, B. *Mater. Sci. Eng., A* **2007**, *444*, 227.

(30) According to the prediction from the Langevin function, using bulk saturation magnetization of 84 emu/g of Fe_3O_4 and magnetic field of 0.35 T, ΔT of 50 K should reduce the magnetization of the nanocrystals by less than 2.5% for the nanocrystals of all sizes in ref 17.